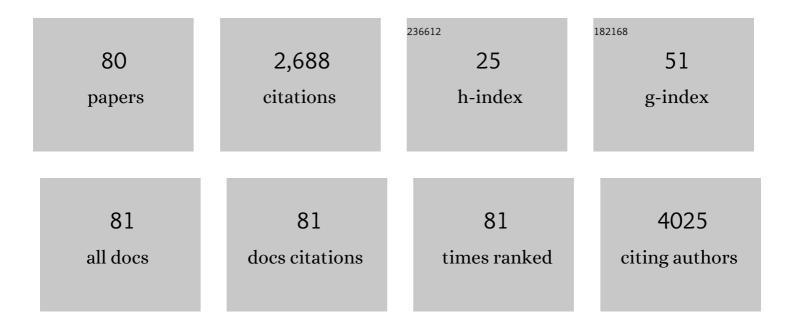
List of Publications by Year in descending order

Source: https://exaly.com/author-pdf/4149121/publications.pdf Version: 2024-02-01



#	Article	lF	CITATIONS
1	<i>In Situ</i> Grown Nanocrystalline Si Recombination Junction Layers for Efficient Perovskite–Si Monolithic Tandem Solar Cells: Toward a Simpler Multijunction Architecture. ACS Applied Materials & Interfaces, 2022, 14, 33505-33514.	4.0	6
2	Insights into Microscopic Crystal Growth Dynamics of CH <sub>3</sub> NH <sub>3</sub> PbI <sub>3</sub> under a Laser Deposition Process Revealed by <i>In Situ</i> X-ray Diffraction. ACS Applied Materials & Interfaces, 2021, 13, 22559-22566.	4.0	3
3	Molecular arrangement in diphenylanthracene derivative films deposited under vacuum on in-plane oriented polythiophene films. Japanese Journal of Applied Physics, 2021, 60, 085504.	0.8	1
4	(Invited) Vacuum Deposition and Crystal Growth of Organolead Halide Perovskite. ECS Meeting Abstracts, 2021, MA2021-02, 640-640.	0.0	0
5	Substrate-driven switchable molecular orientation in bulk heterojunction films identified using infrared reflection absorption spectroscopy. Molecular Systems Design and Engineering, 2020, 5, 559-564.	1.7	5
6	Epitaxial growth of CH3NH3PbI3 on rubrene single crystal. APL Materials, 2020, 8, .	2.2	11
7	Vacuum deposition and crystal growth dynamics of metal halide perovskite. , 2020, , .		Ο
8	Evaluation of exciton diffusion length in highly oriented fullerene films of fullerene/p-Si(100) hybrid solar cells. Japanese Journal of Applied Physics, 2019, 58, 121004.	0.8	1
9	Tuning Methylammonium Iodide Amount in Organolead Halide Perovskite Materials by Post-Treatment for High-Efficiency Solar Cells. ACS Applied Materials & Interfaces, 2019, 11, 38683-38688.	4.0	25
10	Effects of optical interference and optimized crystallinity in organic photovoltaic cells with a low-bandgap small molecule fabricated by dry process. Japanese Journal of Applied Physics, 2019, 58, SBBG12.	0.8	0
11	Oriented thin films of mixture of a low-bandgap polymer and a fullerene derivative prepared by friction-transfer method. Japanese Journal of Applied Physics, 2018, 57, 02CA06.	0.8	2
12	Optical Characteristics and Operational Principles of Hybrid Perovskite Solar Cells. Physica Status Solidi (A) Applications and Materials Science, 2018, 215, 1700730.	0.8	48
13	Semiconducting silicon-tin alloy nanocrystals with direct bandgap behavior for photovoltaic devices. Materials Today Energy, 2018, 7, 87-97.	2.5	15
14	Influence of O <sub>2</sub> plasma treatment on NiO <i> <sub>x</sub> </i> layer in perovskite solar cells. Japanese Journal of Applied Physics, 2018, 57, 04FS07.	0.8	26
15	Effects of solvent vapor annealing on organic photovoltaics with a new type of solution-processable oligothiophene-based electronic donor material. Japanese Journal of Applied Physics, 2018, 57, 08RE09.	0.8	5
16	Organic-Inorganic Hybrid Perovskite Solar Cells. Springer Series in Optical Sciences, 2018, , 463-507.	0.5	2
17	Organic-Inorganic Hybrid Perovskites. Springer Series in Optical Sciences, 2018, , 471-493.	0.5	1
18	Transparent Conductive Oxides. Springer Series in Optical Sciences, 2018, , 495-541.	0.5	1

#	Article	IF	CITATIONS
19	Organic Semiconductors. Springer Series in Optical Sciences, 2018, , 427-469.	0.5	1
20	Organic Photovoltaic Devices Based on Oriented <i>n</i> -Type Molecular Films Deposited on Oriented Polythiophene Films. Journal of Nanoscience and Nanotechnology, 2018, 18, 2702-2710.	0.9	4
21	Tail state formation in solar cell materials: First principles analyses of zincblende, chalcopyrite, kesterite, and hybrid perovskite crystals. Physical Review Materials, 2018, 2, .	0.9	39
22	Universal rules for visible-light absorption in hybrid perovskite materials. Journal of Applied Physics, 2017, 121, .	1.1	91
23	Adjustment of Conduction Band Edge of Compact TiO <sub>2</sub> Layer in Perovskite Solar Cells Through TiCl <sub>4</sub> Treatment. ACS Applied Materials & Interfaces, 2017, 9, 36708-36714.	4.0	35
24	Stable ultrathin surfactantâ€free surfaceâ€engineered silicon nanocrystal solar cells deposited at room temperature. Energy Science and Engineering, 2017, 5, 184-193.	1.9	11
25	Epitaxial Growth of C <sub>60</sub> on Rubrene Single Crystals for a Highly Ordered Organic Donor/Acceptor Interface. Crystal Growth and Design, 2017, 17, 4622-4627.	1.4	17
26	Determination and interpretation of the optical constants for solar cell materials. Applied Surface Science, 2017, 421, 276-282.	3.1	24
27	Hysteresis Analysis of Organolead Halide Perovskite Solar Cells by Transient Current Measurement. Electrochemistry, 2017, 85, 276-279.	0.6	3
28	Constructing Nanostructured Donor/Acceptor Bulk Heterojunctions via Interfacial Templates for Efficient Organic Photovoltaics. ACS Applied Materials & Interfaces, 2017, 9, 43893-43901.	4.0	5
29	Domain structure and electronic state in P3HT:PCBM blend thin films by soft X-ray resonant scattering. Journal of Applied Physics, 2016, 120, .	1.1	1
30	Degradation mechanism of CH3NH3PbI3 perovskite materials upon exposure to humid air. Journal of Applied Physics, 2016, 119, .	1.1	168
31	Relationship between photostability and nanostructures in DTS(FBTTh2)2:fullerene bulk-heterojunction films. Solar Energy Materials and Solar Cells, 2016, 151, 96-101.	3.0	7
32	Highly Controlled Codeposition Rate of Organolead Halide Perovskite by Laser Evaporation Method. ACS Applied Materials & Interfaces, 2016, 8, 26013-26018.	4.0	25
33	Laser deposition for the controlled co-deposition of organolead halide perovskite. , 2016, , .		0
34	Optical Transitions in Hybrid Perovskite Solar Cells: Ellipsometry, Density Functional Theory, and Quantum Efficiency Analyses for <mml:math <br="" xmlns:mml="http://www.w3.org/1998/Math/MathML">display="inline"&gt;<mml:mrow><mml:msub><mml:mrow><mml:mi>CH</mml:mi></mml:mrow><mml:mn>3Physical Review Applied, 2016, 5, .</mml:mn></mml:msub></mml:mrow></mml:math>	ıl:mn> <td>ml<del>322</del> ml:msub&gt;<mi< td=""></mi<></td>	ml <del>322</del> ml:msub> <mi< td=""></mi<>
35	Thermal stabilization of organic photovoltaic cells using [6,6]-phenyl C61-butyric acid methyl ester analogs: Effects of alkyl substituents on the nanostructures of bulk heterojunction films and their stabilities. Synthetic Metals, 2016, 221, 61-66.	2.1	3
36	Fabrication of carbon nanotube hybrid films as transparent electrodes for small-molecule photovoltaic cells. RSC Advances, 2016, 6, 25062-25069.	1.7	10

#	Article	IF	CITATIONS
37	Synthesis of Novel Push–Pull Chromophores based on <i>N</i> -Ethylcarbazole for Vacuum Deposition Processed Organic Photovoltaics. Chemistry Letters, 2015, 44, 958-960.	0.7	5
38	Oriented Thin Films of the Low-Band-Gap Polymer PTB7 by Friction Transfer Method. Molecular Crystals and Liquid Crystals, 2015, 621, 118-123.	0.4	3
39	Crystallization Dynamics of Organolead Halide Perovskite by Real-Time X-ray Diffraction. Nano Letters, 2015, 15, 5630-5634.	4.5	77
40	Understanding Device-Structure-Induced Variations in Open-Circuit Voltage for Organic Photovoltaics. ACS Applied Materials & Interfaces, 2015, 7, 10814-10822.	4.0	2
41	Efficiency limit analysis of organic solar cells: model simulation based on vanadyl phthalocyanine/C60planar junction cell. Japanese Journal of Applied Physics, 2014, 53, 01AB12.	0.8	6
42	Templating Effects in Molecular Growth of Blended Films for Efficient Small-Molecule Photovoltaics. ACS Applied Materials & Interfaces, 2014, 6, 6369-6377.	4.0	28
43	Structural influences on charge carrier dynamics for small-molecule organic photovoltaics. Journal of Applied Physics, 2014, 116, 013105.	1.1	6
44	Heteroepitaxial growth of C <sub>60</sub> on tetracene single crystal. Materials Research Society Symposia Proceedings, 2013, 1501, 1.	0.1	6
45	Control of neural signal propagation in neuron by three terminal electrodes method. Electronics Letters, 2012, 48, 1093-1095.	0.5	0
46	Extended Exciton Diffusion in Rubrene Single-Crystalline Organic Solar Cells. Materials Research Society Symposia Proceedings, 2012, 1390, 89.	0.1	5
47	Structural modifications of zinc phthalocyanine thin films for organic photovoltaic applications. Journal of Applied Physics, 2012, 111, .	1.1	13
48	Phase separation of co-evaporated ZnPc:C60 blend film for highly efficient organic photovoltaics. Applied Physics Letters, 2012, 100, 233302.	1.5	50
49	Glancing Angle Deposition of Copper Iodide Nanocrystals for Efficient Organic Photovoltaics. Nano Letters, 2012, 12, 4146-4152.	4.5	92
50	Analytical model for the design principle of large-area solar cells. Solar Energy Materials and Solar Cells, 2012, 97, 127-131.	3.0	13
51	Controlled growth of dibenzotetraphenylperiflanthene thin films by varying substrate temperature for photovoltaic applications. Solar Energy Materials and Solar Cells, 2011, 95, 2861-2866.	3.0	20
52	Controlled growth off ZnPc thin filmss for phootovoltaic appplications. Physics Procedia, 2011, 14, 221-225.	1.2	3
53	Mg <sub>x</sub> C <sub>60</sub> Fabricated by Using Mg:C <sub>60</sub> Co-Evaporation Method for Carrier Doping. Molecular Crystals and Liquid Crystals, 2011, 538, 193-198.	0.4	2
54	Pulsed Bias Stress in Pentacene Thin Film Transistors and Effect of Contact Material. Japanese Journal of Applied Physics, 2010, 49, 01AB03.	0.8	2

#	Article	IF	CITATIONS
55	Contact resistance instability in pentacene thin film transistors induced by ambient gases. Applied Physics Letters, 2009, 94, 083309.	1.5	18
56	Surface selective deposition of molecular semiconductors for solution-based integration of organic field-effect transistors. Applied Physics Letters, 2009, 94, .	1.5	96
57	Thinâ€film transistors fabricated from semiconductorâ€enriched singleâ€wall carbon nanotubes. Physica Status Solidi (B): Basic Research, 2009, 246, 2849-2852.	0.7	3
58	Simple and Scalable Gel-Based Separation of Metallic and Semiconducting Carbon Nanotubes. Nano Letters, 2009, 9, 1497-1500.	4.5	307
59	Bias stress instability in pentacene thin film transistors: Contact resistance change and channel threshold voltage shift. Applied Physics Letters, 2008, 92, 063305.	1.5	90
60	Charge trapping induced current instability in pentacene thin film transistors: Trapping barrier and effect of surface treatment. Applied Physics Letters, 2008, 93, .	1.5	78
61	Dynamic bias stress current instability caused by charge trapping and detrapping in pentacene thin film transistors. Applied Physics Letters, 2008, 93, .	1.5	13
62	Selective organization of solution-processed organic field-effect transistors. Applied Physics Letters, 2008, 92, .	1.5	74
63	Correlation between grain size and device parameters in pentacene thin film transistors. Applied Physics Letters, 2008, 93, .	1.5	93
64	Analysis of charge transport in a polycrystalline pentacene thin film transistor by temperature and gate bias dependent mobility and conductance. Journal of Applied Physics, 2007, 102, .	1.1	64
65	Contact-metal dependent current injection in pentacene thin-film transistors. Applied Physics Letters, 2007, 91, .	1.5	137
66	Frequency response analysis of pentacene thin-film transistors with low impedance contact by interface molecular doping. Applied Physics Letters, 2007, 91, .	1.5	55
67	Suppression of short channel effect in organic thin film transistors. Applied Physics Letters, 2007, 91, .	1.5	53
68	Charge injection process in organic field-effect transistors. Applied Physics Letters, 2007, 91, .	1.5	140
69	Scaling effect on the operation stability of short-channel organic single-crystal transistors. Applied Physics Letters, 2007, 91, 063506.	1.5	16
70	Current transport in short channel top-contact pentacene field-effect transistors investigated with the selective molecular doping technique. Applied Physics Letters, 2007, 90, 193507.	1.5	62
71	Investigation of complex channel capacitance in C60 field effect transistor and evaluation of the effect of grain boundaries. Current Applied Physics, 2007, 7, 87-91.	1.1	10
72	Anisotropic Polymerization of a Long-Chain Diacetylene Derivative Langmuirâ^'Blodgett Film on a Step-Bunched SiO2/Si Surface. Langmuir, 2006, 22, 5742-5747.	1.6	7

#	Article	IF	CITATIONS
73	In-situ measurement of molecular orientation of the pentacene ultrathin films grown on SiO2 substrates. Surface Science, 2006, 600, 2518-2522.	0.8	27
74	Thickness Dependent Characteristics of a Copper Phthalocyanine Thin-Film Transistor Investigated by in situ FET Measurement System. Molecular Crystals and Liquid Crystals, 2006, 455, 347-351.	0.4	9
75	Analysis of transient phenomena of C60 field effect transistors. Applied Physics Letters, 2006, 89, 172117.	1.5	11
76	Accelerated photopolymerization and increased mobility in C60 field-effect transistors studied by ultraviolet photoelectron spectroscopy. Applied Physics Letters, 2004, 84, 2439-2441.	1.5	7
77	Methyl-terminated Si(111) surface as the ultra thin protection layer to fabricate position-controlled alkyl SAMs by using atomic force microscope anodic oxidation. Surface Science, 2004, 552, 46-52.	0.8	11
78	Band Structure and Molecular Orientation of Ultrathin Epitaxial Films of Squaric Acid. Journal of Physical Chemistry B, 2004, 108, 5329-5332.	1.2	2
79	Ultraviolet photoelectron spectroscopy of a methyl-terminated Si surface. Surface Science, 2003, 526, 177-183.	0.8	21
80	Performance Enhancement of Thin-Film Transistors by Using High-Purity Semiconducting Single-Wall Carbon Nanotubes. Applied Physics Express, 0, 2, 071601.	1.1	33